

A bacteriophage nucleus-like compartment shields DNA from CRISPR nucleases

<https://doi.org/10.1038/s41586-019-1786-y>

Received: 16 July 2018

Accepted: 11 October 2019

Published online: 09 December 2019

Senén D. Mendoza¹, Eliza S. Nieweglowska^{2,7}, Sutharsan Govindarajan^{1,5,7}, Lina M. Leon¹, Joel D. Berry¹, Anika Tiwari¹, Vorrapon Chaikerasitak^{3,6}, Joe Pogliano³, David A. Agard^{2,4} & Joseph Bondy-Denomy^{1,4*}

All viruses require strategies to inhibit or evade the immune pathways of cells that they infect. The viruses that infect bacteria, bacteriophages (phages), must avoid immune pathways that target nucleic acids, such as CRISPR–Cas and restriction-modification systems, to replicate efficiently¹. Here we show that jumbo phage Φ KZ segregates its DNA from immunity nucleases of its host, *Pseudomonas aeruginosa*, by constructing a proteinaceous nucleus-like compartment. Φ KZ is resistant to many immunity mechanisms that target DNA in vivo, including two subtypes of CRISPR–Cas3, Cas9, Cas12a and the restriction enzymes HsdRMS and EcoRI. Cas proteins and restriction enzymes are unable to access the phage DNA throughout the infection, but engineering the relocalization of EcoRI inside the compartment enables targeting of the phage and protection of host cells. Moreover, Φ KZ is sensitive to Cas13a—a CRISPR–Cas enzyme that targets RNA—probably owing to phage mRNA localizing to the cytoplasm. Collectively, we propose that *Pseudomonas* jumbo phages evade a broad spectrum of DNA-targeting nucleases through the assembly of a protein barrier around their genome.

Phages that infect *Pseudomonas aeruginosa* can avoid destruction mediated by CRISPR by encoding ‘anti-CRISPR’ proteins that inhibit the type I-E and I-F CRISPR–Cas systems^{2–4}. To determine whether any *P. aeruginosa* phages are resistant to the *P. aeruginosa* type I-C CRISPR–Cas system⁵ (a common, but understudied variant⁶), we engineered a strain of *P. aeruginosa* to express type I-C *cas3*, *cas5*, *cas8* and *cas7*, and provided this strain with a panel of CRISPR RNAs (crRNAs) that target phages from five taxonomic groups: JBD30, D3, JBD68 (distinct temperate siphophages), F8 and Φ KZ (distinct lytic myophages). All phages succumbed to targeting (Fig. 1a), except for Φ KZ (Fig. 1b) and a related phage, Φ PA3 (Extended Data Fig. 1a). The Φ KZ titre did not decrease when Φ KZ was challenged with 11 different type I-C crRNAs (Fig. 1b, Extended Data Fig. 2a), nor when it was targeted by the type I-F CRISPR–Cas system of *P. aeruginosa*⁸ (Extended Data Fig. 2b).

Phage Φ KZ resists CRISPR–Cas targeting

The Φ KZ genome has no homologues of known anti-CRISPR (Acr) genes^{2–4,9,10}, or anti-CRISPR-associated genes, which have previously enabled identification of Acr genes^{4,9,10}. Moreover, gene knockout approaches have not been established for Φ KZ. Therefore, to determine the mechanism by which this phage can evade CRISPR-mediated destruction we used type II-A CRISPR–Cas9 from *Streptococcus pyogenes* (*SpyCas9*). *SpyCas9* and single-guide RNAs (sgRNAs) robustly targeted control phage JBD30, but phage replication and the associated lysis of host cells were unaffected during phage Φ KZ infection (Fig. 1c). An additional six sgRNA sequences were also unable to impact Φ KZ

replication (Extended Data Fig. 3a), as were four sgRNAs against Φ PA3 (Extended Data Fig. 1b). Given the ability of this phage to evade unrelated CRISPR systems (types I and II)—including one from a microorganism that this phage does not infect (*S. pyogenes*)—we hypothesized that Φ KZ might be generally resistant to CRISPR–Cas immunity, as opposed to relying on specific inhibitor proteins. When we expressed the type V-A Cas12a (Cpf1) CRISPR–Cas system from *Moraxella bovoculi* in *P. aeruginosa*, the control phage was targeted successfully, but Φ KZ was not, with any of the nine crRNAs tested (Fig. 1d, Extended Data Fig. 3b). The ability of Φ KZ to resist both CRISPR systems that are found in its natural host, *Pseudomonas* (types I-C and I-F), and those that are not naturally present in *Pseudomonas* (types II-A and V-A) suggests that this phage has a mechanism that enables ‘pan-CRISPR’ resistance.

Restriction-modification (R-M) systems are the most common form of bacterial immunity in nature and pose a substantial impediment to phage replication¹. We next tested type I and type II R-M systems (HsdRMS from *P. aeruginosa* and EcoRI from *Escherichia coli*, respectively; 24 and 92 cut sites in the Φ KZ genome, respectively). Φ KZ was propagated on the *P. aeruginosa* strain PAK, an isolate that generates phages that are susceptible to HsdRMS restriction when infecting the PAO1 strain. When phage JBD30 (which has five type I R-M sites) was assayed in this manner, its titre was reduced by five orders of magnitude, which was dependent on *hsdR* (Fig. 1e). By contrast, no restriction was observed for Φ KZ (Fig. 1e) or Φ PA3 (Extended Data Fig. 1c). Similarly, the expression of EcoRI reduced the titre of JBD30 (6 EcoRI sites) by three orders of magnitude, but had no effect on Φ KZ (92 EcoRI sites) (Fig. 1f). Together, these experiments demonstrate that Φ KZ is

¹Department of Microbiology and Immunology, University of California San Francisco, San Francisco, CA, USA. ²Howard Hughes Medical Institute, Department of Biochemistry and Biophysics, University of California San Francisco, San Francisco, CA, USA. ³Division of Biological Sciences, University of California San Diego, La Jolla, CA, USA. ⁴Quantitative Biosciences Institute, University of California San Francisco, San Francisco, CA, USA. ⁵Present address: Department of Biology, SRM University AP, Amaravati, India. ⁶Present address: Department of Biochemistry, Faculty of Science, Chulalongkorn University, Bangkok, Thailand. ⁷These authors contributed equally: Eliza S. Nieweglowska, Sutharsan Govindarajan. *e-mail: Joseph.Bondy-Denomy@ucsf.edu

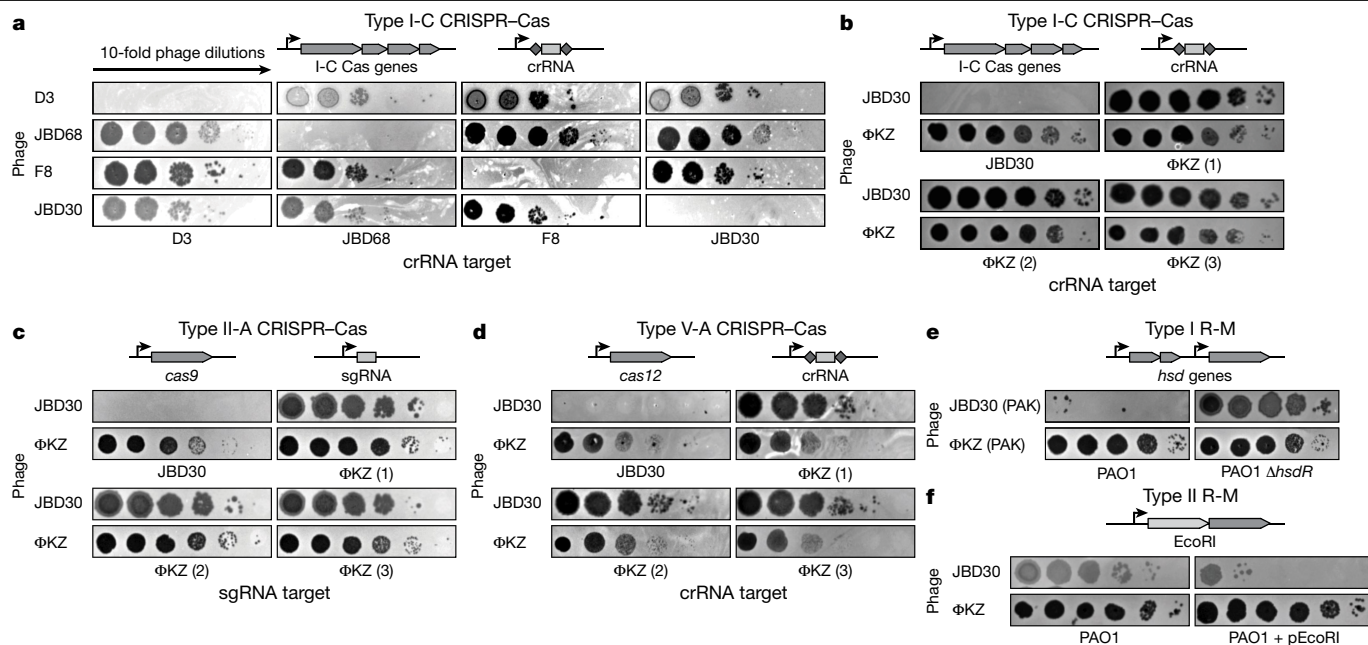


Fig. 1 | Identification of a phage that resists targeting by diverse CRISPR–Cas and R–M systems. Plaque assays with the indicated phage spotted in tenfold serial dilutions on a lawn of *P. aeruginosa*; dark clearings in the lawn represent phage replication. **a–d**, Strain PAO1 expressing type I–C Cas genes (*cas3*, *cas5*, *cas8*, *cas7*) and crRNAs that target the indicated phages (**a**); type I–C Cas genes and crRNAs that target phage JBD30 or distinct crRNAs (1–3) that target phage ΦKZ (**b**); type II–A *cas9* and distinct sgRNAs that target the indicated phages (**c**); or type V–A *cas12a* and distinct crRNAs against the

indicated phages (**d**). **e**, An endogenous type I R–M system (*hsdRSM*) in wild-type PAO1 and a mutant strain with an isogenic *hsdR* knockout (PAO1 Δ *hsdR*) was assayed using phages that were propagated on PAK (for example, JBD30 (PAK) was first propagated on strain PAK). **f**, The type II EcoRI R–M system in PAO1. Restriction activity was assayed using phages JBD30 and ΦKZ. pEcoRI denotes plasmid-expressed EcoRI. All plaque assays were replicated two or more times with similar results.

refractory to our six selected CRISPR–Cas (types I–C, I–F, II–A, and V–A) and restriction endonucleases (types I and II) in vivo.

Protein barrier occludes immune enzymes

ΦKZ and ΦKZ-like phages that infect *P. aeruginosa* and *Pseudomonas chlororaphis* have been shown to construct an elaborate proteinaceous nucleus-like compartment in which the replication of phage DNA takes place^{11,12}. In addition, a phage-encoded homologue of tubulin, PhuZ, centres the compartment within the host cell^{11–15}. Proteins that are involved in DNA replication, transcription and recombination localize inside the shell, whereas mRNA and proteins that mediate translation localize in the cytoplasmic space¹¹—similarly to the eukaryotic nucleus. Given the apparent exclusion of specific proteins, we hypothesized that this structure might be responsible for the pan-resistance of ΦKZ to distinct immune processes.

P. aeruginosa cells that were infected with ΦKZ were imaged with immunofluorescence to detect Cas9 (Fig. 2a, Extended Data Fig. 4). We also used live-cell imaging to detect Cherry fusions with Cas9, two signature proteins from the type I–C and I–F CRISPR–Cas systems (Cas8 and Cas3; Fig. 2b) and the restriction enzyme HsdR (Fig. 2c). These experiments showed that the immune enzymes are excluded from the shell during phage infection. DAPI staining revealed that the phage DNA was located inside the shell, whereas the host genome was degraded¹⁴. The phage protein ORF152 (imaged with anti-Myc immunofluorescence and Cherry fusion) and host protein topoisomerase I (Cherry fusion)—both of which have been previously shown to be internalized in the shell—colocalized with the DAPI signal, but Cherry was excluded (Fig. 2d). Although the rules that govern protein internalization in the shell are currently unknown, each protein of known function that localizes inside the shell interacts with DNA^{11,12} (that is, forms part of the DNA replication and transcription machinery), suggesting that the

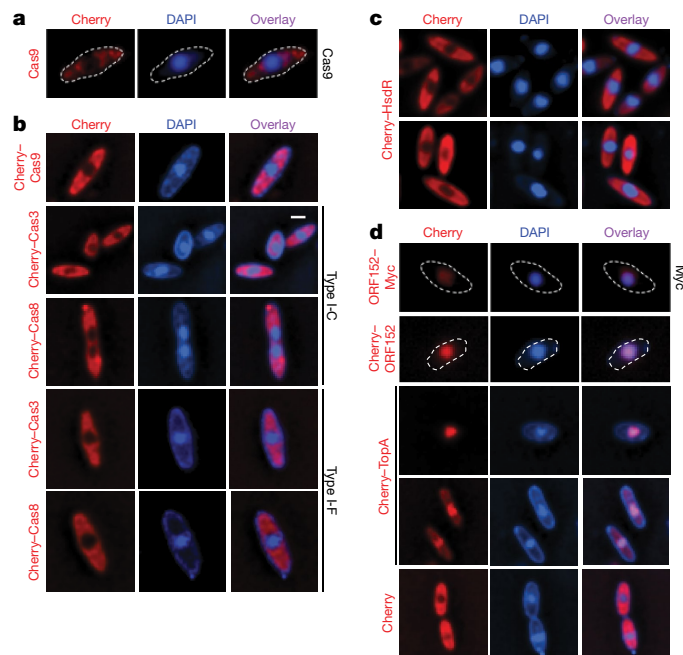


Fig. 2 | CRISPR–Cas proteins and restriction enzymes are excluded from the nucleus-like structure of ΦKZ. **a**, Fluorescence microscopy of *P. aeruginosa*, immunostained for Cas9. The DAPI stain shows the phage DNA within the nucleus-like structure. **b, c**, Live-cell fluorescence imaging of *P. aeruginosa* strains that were engineered to express type II–A Cas9, type I–C or I–F Cas8 or Cas3 proteins fused to Cherry (**b**) or HsdR fused to Cherry (**c**). Scale bar, 1 μm. **d**, Top row, fluorescence microscopy of Myc-tagged ORF152 in *P. aeruginosa*, imaged with anti-Myc immunofluorescence. Bottom rows, live-cell fluorescence imaging of ORF152 and TopA proteins fused to Cherry, or Cherry alone. All experiments were replicated two or more times with similar results.

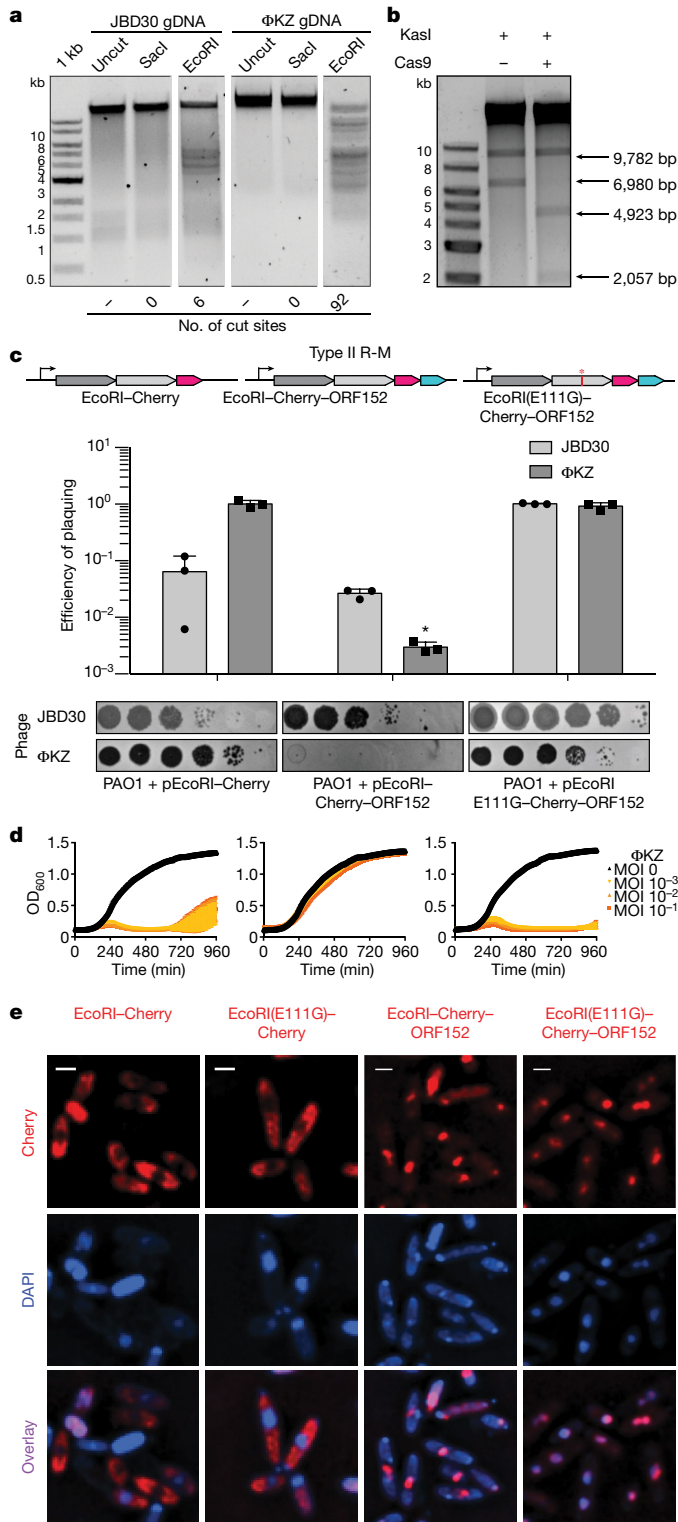


Fig. 3 Φ KZ gDNA can be cleaved by immune enzymes. **a**, Φ KZ and JBD30 gDNA digested with the indicated restriction enzymes *in vitro*. The first lane contains a 1-kb DNA ladder. The number of cut sites for each enzyme is shown at the bottom of the gels. Products were visualized on a 0.7% agarose gel stained with the DNA stain SYBR Safe. **b**, Φ KZ gDNA digested *in vitro* using KasI, and incubated with or without Cas9 loaded with crRNA:tracrRNA that targets the fragment liberated by KasI. Products were visualized on a 0.7% agarose gel stained with SYBR Safe. **c**, Plaque assays for strain PAO1 expressing the fusion proteins EcoRI-Cherry, EcoRI-Cherry-ORF152 or EcoRI(E111G)-Cherry-ORF152. Plaque assays were conducted as in Fig. 1a and quantified ($n = 3$). Data are mean \pm s.d. A Student's *t*-test comparing the efficiency of plaquing of Φ KZ on PAO1 that expresses pEcoRI-Cherry to PAO1 that expresses pEcoRI-Cherry-ORF152 yielded a *P* value of 2.88×10^{-4} (indicated with an asterisk). **d**, Growth curves measuring the optical density at 600 nm (OD_{600nm}) of PAO1 cells that were infected with Φ KZ at the indicated multiplicity of infection (MOI). **e**, Live-cell fluorescence imaging of infected strains of *P. aeruginosa* that were engineered to express EcoRI-Cherry, EcoRI(E111G)-Cherry, EcoRI-Cherry-ORF152 or EcoRI(E111G)-Cherry-ORF152. The DAPI stain shows the phage DNA. The *in vitro* digestion experiments in **a**, **b** were replicated twice with similar results. The plaque assays (**c**), growth curves (**d**) and microscopy (**e**) were replicated three times. Scale bars, 1 μ m.

Owing to the large size of the Φ KZ genome (280 kb), we first subjected purified phage DNA to the restriction enzyme KasI to yield a 6.98-kb product, and then cleaved that species with a *Spy*Cas9 nuclease loaded with both crRNA and trans-activating crRNA (tracrRNA) *in vitro*. This reaction depleted the substrate and produced the expected 4.9-kb and 2.1-kb fragments, confirming that the phage gDNA is sensitive to Cas9 cleavage (Fig. 3b). Together, these results demonstrate that immune enzymes are capable of cleaving Φ KZ gDNA when they can access it, and that immune evasion is probably not a result of an intrinsic feature of the phage DNA (such as base modifications that can impede the Cascade-Cas3 complex, Cas9 and EcoRI)^{16–19}.

Phage targeting via enzyme localization

As there is no currently known method that can be used to mutate, weaken or knockout the phage shell structure, we next sought to enable an immune enzyme to bypass the shell and thereby access the phage DNA *in vivo*. We fused the single effector enzyme Cas9 to ORF152, a phage-encoded RecA-like protein that is internalized within the shell^{11,12}. Independent fusions of Cas9 to the N or the C terminus of ORF152 did not affect the replication of Φ KZ (Extended Data Fig. 6a, b). Imaging of one orientation of ORF152-Cas9 revealed peri-shell localization (Extended Data Fig. 6c, d); this suggests that the fusion redirected Cas9 from its previously diffuse state but that the large Cas9 protein (1,368 amino acids, 158 kDa) was unable to traverse the shell border.

Given the large size (for example, Cas12a) and complexity (for example, Cascade, HsdRMS) of each of the other immune effectors, we next fused the small, single effector protein EcoRI (278 amino acids, 31.5 kDa) to Cherry-tagged ORF152. This fusion resulted in a notable decrease of more than 2.5 orders of magnitude in the Φ KZ titre and markedly reduced plaque sizes (Fig. 3c). Liquid infections revealed that cells that express EcoRI-Cherry-ORF152 were extremely well protected, gaining an increase of more than five orders of magnitude in their resistance to phage-induced lysis (Fig. 3d). A catalytic mutant EcoRI(E111G) fused to Cherry-ORF152 exhibited no immune activity against Φ KZ in either assay, and nor did active EcoRI-Cherry without the ORF152 fusion (Fig. 3c, d). Similar results were observed in the absence of the Cherry tag (that is, EcoRI-ORF152); however, Φ KZ targeting was more modest in that case, reducing titres by approximately tenfold and protecting cells by a factor of around 10^4 (Extended Data Fig. 7). Imaging of infected cells that express EcoRI-Cherry or EcoRI(E111G)-Cherry demonstrated that these proteins are excluded from the shell, whereas EcoRI(E111G)-Cherry-ORF152 is successfully localized inside (Fig. 3e;

exclusion of DNA-binding Cas and restriction proteins is an adaptive function of the shell.

To confirm that the Φ KZ phage genome could be a substrate for DNA cleavage, if accessed, two enzymes that did not cleave Φ KZ *in vivo*, EcoRI and Cas9, were assayed *in vitro*. Φ KZ DNA was extracted from virions and subjected to restriction digestion reactions with a panel of restriction enzymes. EcoRI, HindIII, KpnI and NcoI all cleaved the DNA, whereas SmaI—which lacks a sequence-recognition motif in the Φ KZ genome—did not (Fig. 3a, Extended Data Fig. 5a). The ability of Cas9 to cleave Φ KZ genomic DNA (gDNA) *in vitro* was next assessed.

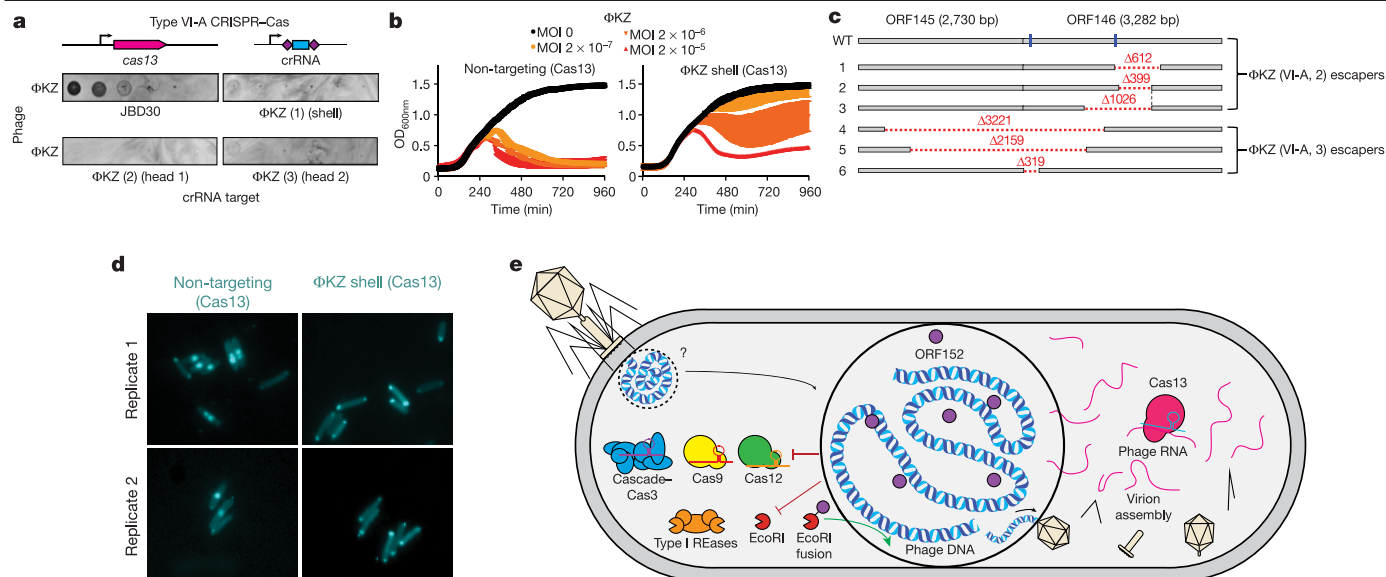


Fig. 4 | Phage ΦKZ DNA is sensitive to RNA targeting with Cas13. **a**, Strain PAOI expressing *LseCas13a* and distinct crRNAs that target the shell (one crRNA) or the head (two crRNAs) of phage ΦKZ. Plaque assays were conducted as in Fig. 1a. **b**, Growth curves measuring the OD_{600nm} of PAOI cells that were infected with ΦKZ at the indicated MOI. **c**, Wild-type (WT) and Cas13 escaper ΦKZ phage, with deletions indicated with red dashed lines and target sites with blue lines. **d**, Live-cell fluorescence imaging of *P. aeruginosa* strains that were engineered to express *LseCas13a* and crRNAs that target ΦKZ. The cyan stain shows the DAPI-stained phage DNA. **e**, Summary model. The ΦKZ nucleus-like

structure excludes Cas9, Cas12, Cascade-Cas3 (type I-C and type I-F), type I restriction endonucleases (REase) and type II restriction endonucleases (for example, EcoRI); however, the mRNA (red) is exported and can be targeted by Cas13. The nucleus-like structure is resistant to the indicated nucleases, but fusing EcoRI to the internal protein ORF152 enables targeting. The assays in **a** were replicated more than three times with similar results. The growth curve experiments (**b**) were replicated twice with similar results. Escaper mutants (**c**) were isolated once and verified by PCR, sequencing and plaque assays. Microscopy (**d**) was replicated twice with similar results.

see Supplementary Video 1 for time-lapse images). EcoRI-Cherry-ORF152 impaired the ability of infected cells to form full shells and proceed through the infection process, and the EcoRI fusion protein was often localized within or adjacent to the DAPI-stained puncta (Fig. 3e, Supplementary Video 2). Some host DNA can be seen in these cells and infection does not proceed (Fig. 3e, Extended Data Fig. 7c, d). By bypassing the physical barrier of the shell using rational engineering, we conclude that the shell is the cause of the resistance to immunity that is shown by jumbo phage ΦKZ.

Phage mRNA is sensitive to Cas13a

The nucleus-like structure produced by ΦKZ provides robust resistance to DNA-targeting immune pathways, but other immune systems may exist in vivo that can evade this mechanism. We envisaged that the mRNA that is exported for translation in the cytoplasm is probably susceptible to targeting and that a ribonuclease could provide anti-ΦKZ immunity. To test this, we adapted the type VI-A CRISPR RNA-guided RNA nuclease Cas13a from *Listeria seeligeri* (*LseCas13a*)^{20,21} for phage targeting in *P. aeruginosa*. Three *LseCas13a* spacers (two targeting the head gene *gp146* and one targeting the shell gene *gp054*) decreased the efficiency of ΦKZ plaquing by more than 10⁶ fold (Fig. 4a, Extended Data Fig. 8). Corroborating these results, *LseCas13a* was also effective at protecting *P. aeruginosa* in liquid cultures, with an increase of 1–2 orders of magnitude in resistance to phage-induced lysis (Fig. 4b). We suspect that the previously demonstrated collateral damage caused by Cas13a²² is detrimental to cell fitness, which leads to an enhancement of the growth curves that is modest compared to that brought about by EcoRI targeting. Cas13 escaper phages (that is, phages that evaded Cas13-mediated targeting) were also identified (Extended Data Fig. 9); these occurred at a frequency of around 10⁻⁶ to 10⁻⁷ and, surprisingly, contained genomic deletions at the site of targeting (Fig. 4c). Notably, all deletions were in-frame and five out of six escaper phages had clear

regions of microhomology flanking the deletion that ranged from 7–21 bp in length. One guide RNA targeting the 5' end of *orf146* selected for deletions in which the upstream gene (*orf145*) became fused, in frame, to the targeted gene (Fig. 4c). These data support the conclusion that sequence-specific RNA targeting by CRISPR-Cas proteins can inhibit this phage.

Before the construction of the shell takes place, the state of the phage DNA is unknown. During Cas13a targeting of the shell mRNA, imaging revealed that infections arrested before the phage DNA proceeded from its injection site at the poles. Most cells had two polar puncta, even one hour after infection (Fig. 4d). The absence of diffusion or clearance of the phage DNA (for example, by the endogenous type I R-M system) suggests that the injected phage genome may be protected before shell assembly by injected phage proteins or pre-existing host factors. The potential for a DNA structure to exist prior to shell construction is further corroborated by our observation that in the absence of Cas13a-mediated arrest, DAPI-stained phage DNA was detected adjacent to EcoRI-Cherry-ORF152 puncta (Fig. 3e) or adjacent to a nascent shell in which TopA was localized (Extended Data Fig. 10). The molecular nature and mechanisms underlying this early protection event remain to be elucidated.

Discussion

The assembly of a proteinaceous compartment in which phage DNA replication occurs creates a physical protective barrier that results in the resistance of phage ΦKZ to enzymes that cleave DNA (Fig. 4e). The evasion of endogenous *P. aeruginosa* type I CRISPR-Cas systems by ΦKZ suggests that these jumbo phages are probably resistant to type I CRISPR-Cas systems in nature. Supporting this hypothesis, our analysis of a previously published collection of over 4,000 non-redundant *P. aeruginosa* spacers⁵ (types I-C, I-E and I-F) found no spacers against ΦKZ or its jumbo phage relatives ΦPA3, PaBg, KTN4 and PA7

Table 1 | No spacers against Φ KZ-like phages

Phage	No. of spacers	Type I CRISPR sensitivity	Reference
DMS3m	75	I-C: sensitive; I-E: resistant (AcrIE3); I-F: sensitive	This study and previous studies ^{3,8}
JBD30	51	I-C: sensitive; I-E: sensitive; I-F: resistant (AcrIF1)	This study and previous studies ^{2,3}
JBD18	51	I-F: sensitive	A previous study ⁸
JBD25	46	I-F: sensitive	A previous study ⁸
JBD68	28	I-C: sensitive	This study
D3	49	I-C: sensitive	This study
F8	3	I-C: sensitive	This study
Φ KZ	0	I-C: resistant; I-F: resistant	This study
phiPA3	0	I-C: resistant	This study
PaBG	0	not assayed	
KTN4	0	not assayed	
PA7	0	not assayed	

The total number of type I CRISPR spacers with a perfect match to the indicated *P. aeruginosa* phages assayed in this study and previous CRISPR–Cas studies. The experimental sensitivity of each phage to the indicated subtypes is shown. AcrIE3 and AcrIF1 are I-E and I-F anti-CRISPR proteins, respectively. For F8, the 3 spacers have mismatches (4 nucleotides or fewer) to the F8 genome.

(Table 1). By contrast, many spacers from each system match diverse *P. aeruginosa* phages, such as those assayed in our screen (Fig. 1) and those encoding anti-CRISPR proteins. In addition, given the efficacy of the RNA-targeting CRISPR–Cas13 system, we propose that type VI CRISPR systems are well suited to target the mRNA of DNA phages when the DNA is inaccessible (that is, owing to base modifications or physical segregation).

Although this phage compartment has only been documented among the jumbo phages of *Pseudomonas*^{11,12}, physical occlusion of phage gDNA through this and other mechanisms may constitute a route through which immune systems can be evaded by other phages. Indeed, ‘mega phages’ have recently been reported to encode homologues of phage tubulin, which in *Pseudomonas* are involved in centring the proteinaceous compartment during infection²³. The pan-resistance of Φ KZ to enzymes that target DNA provides an explanation for the elaborate, nucleus-like structure. Furthermore, the polar localization of the injected phage DNA during mRNA targeting suggests a poorly understood early protective mechanism. Considering the pronounced resistance to overexpressed immune enzymes and the previously observed docking of capsids at the shell periphery^{11,24}, we propose that the phage DNA is never exposed to the cytoplasm (Fig. 4e). Other hypotheses to explain the importance of the shell—including protection from phage-derived nucleases that degrade the bacterial genome, and spatial organization of the large phage genome during replication and packaging—remain to be addressed. Regardless, we conclude that the phage-assembled nucleus-like structure provides a strong protective barrier to DNA-targeting immune pathways.

Online content

Any methods, additional references, Nature Research reporting summaries, source data, extended data, supplementary information, acknowledgements, peer review information; details of author contributions and competing interests; and statements of data and code availability are available at <https://doi.org/10.1038/s41586-019-1786-y>.

- Koonin, E. V., Makarova, K. S. & Wolf, Y. I. Evolutionary genomics of defense systems in archaea and bacteria. *Annu. Rev. Microbiol.* **71**, 233–261 (2017).
- Bondy-Denomy, J., Pawluk, A., Maxwell, K. L. & Davidson, A. R. Bacteriophage genes that inactivate the CRISPR/Cas bacterial immune system. *Nature* **493**, 429–432 (2013).
- Pawluk, A., Bondy-Denomy, J., Cheung, V. H. W., Maxwell, K. L. & Davidson, A. R. A new group of phage anti-CRISPR genes inhibits the type I-E CRISPR–Cas system of *Pseudomonas aeruginosa*. *MBio* **5**, e00896-e14 (2014).
- Pawluk, A. et al. Inactivation of CRISPR–Cas systems by anti-CRISPR proteins in diverse bacterial species. *Nat. Microbiol.* **1**, 16085 (2016).
- van Belkum, A. et al. Phylogenetic distribution of CRISPR–Cas systems in antibiotic-resistant *Pseudomonas aeruginosa*. *MBio* **6**, e01796-e15 (2015).
- Makarova, K. S. et al. An updated evolutionary classification of CRISPR–Cas systems. *Nat. Rev. Microbiol.* **13**, 722–736 (2015).
- Marino, N. D. et al. Discovery of widespread type I and type V CRISPR–Cas inhibitors. *Science* **362**, 240–242 (2018).
- Cady, K. C., Bondy-Denomy, J., Heussler, G. E., Davidson, A. R. & O’Toole, G. A. The CRISPR/Cas adaptive immune system of *Pseudomonas aeruginosa* mediates resistance to naturally occurring and engineered phages. **194**, 5728–5738 (2012).
- Pawluk, A. et al. Naturally occurring off-switches for CRISPR–Cas9. *Cell* **167**, 1829–1838 (2016).
- Rauch, B. J. et al. Inhibition of CRISPR–Cas9 with bacteriophage proteins. *Cell* **168**, 150–158 (2017).
- Chaikeeratisak, V. et al. Assembly of a nucleus-like structure during viral replication in bacteria. *Science* **355**, 194–197 (2017).
- Chaikeeratisak, V. et al. The phage nucleus and tubulin spindle are conserved among large *Pseudomonas* phages. *Cell Rep.* **20**, 1563–1571 (2017).
- Kraemer, J. A. et al. A phage tubulin assembles dynamic filaments by an atypical mechanism to center viral DNA within the host cell. *Cell* **149**, 1488–1499 (2012).
- Erb, M. L. et al. A bacteriophage tubulin harnesses dynamic instability to center DNA in infected cells. *eLife* **3**, e03197 (2014).
- Zehr, E. A. et al. The structure and assembly mechanism of a novel three-stranded tubulin filament that centers phage DNA. *Structure* **22**, 539–548 (2014).
- Bryson, A. L. et al. Covalent modification of bacteriophage T4 DNA inhibits CRISPR–Cas9. *MBio* **6**, e00648-15 (2015).
- Strotskaya, A. et al. The action of *Escherichia coli* CRISPR–Cas system on lytic bacteriophages with different lifestyles and development strategies. *Nucleic Acids Res.* **45**, 1946–1957 (2017).
- Vlot, M. et al. Bacteriophage DNA glucosylation impairs target DNA binding by type I and II but not by type V CRISPR–Cas effector complexes. *Nucleic Acids Res.* **46**, 873–885 (2018).
- Huang, L. H., Farnet, C. M., Ehrlich, K. C. & Ehrlich, M. Digestion of highly modified bacteriophage DNA by restriction endonucleases. *Nucleic Acids Res.* **10**, 1579–1591 (1982).
- Abudayyeh, O. O. et al. C2c2 is a single-component programmable RNA-guided RNA-targeting CRISPR effector. *Science* **353**, aaf5573 (2016).
- Gootenberg, J. S. et al. Nucleic acid detection with CRISPR–Cas13a/C2c2. *Science* **356**, 438–442 (2017).
- Meeske, A. J. & Marraffini, L. A. RNA guide complementarity prevents self-targeting in type VI CRISPR systems. *Mol. Cell* **71**, 791–801 (2018).
- Al-Shayeb, B. et al. Clades of huge phage from across Earth’s ecosystems. Preprint at *bioRxiv* <https://www.biorxiv.org/content/10.1101/572362v1> (2019).
- Chaikeeratisak, V. et al. Viral capsid trafficking along treadmilling tubulin filaments in bacteria. *Cell* **177**, 1771–1780 (2019).

Publisher’s note Springer Nature remains neutral with regard to jurisdictional claims in published maps and institutional affiliations.

© The Author(s), under exclusive licence to Springer Nature Limited 2019

Article

Methods

No statistical methods were used to predetermine sample size. The experiments were not randomized, and investigators were not blinded to allocation during experiments and outcome assessment.

Bacterial growth and genetic manipulation

The strains, plasmids, phages and spacer sequences used in this study are listed in the Supplementary Information. *P. aeruginosa* strain PAO1 was grown in LB at 37 °C with aeration at 225 rpm. When necessary, plating was performed on LB agar with carbenicillin (250 µg ml⁻¹) or gentamicin (50 µg ml⁻¹). Gene expression was induced by the addition of L-arabinose (0.1% final) and/or isopropyl β-D-1-thiogalactopyranoside (IPTG; 0.5 mM or 1 mM final). For chromosomal insertions at the attTn7 locus, *P. aeruginosa* cells were electroporated with the integrating vector pUC18T-lac and the transposase expressing helper plasmid pTNS3, and selected on gentamicin. Potential integrants were screened by colony PCR with primers PTn7R and PglmS-down. Electrocompetent cell preparations, transformations, integrations, selections, plasmid curing and FLP-recombinase-mediated marker excision with pFLP were performed as described previously²⁵.

Phage growth and DNA extraction

Phage growth was conducted in LB at 37 °C with PAO1 as a host. Growth curves were conducted in a Biotek Synergy plate reader at 37 °C with orbital shaking set to maximum speed. Phage stocks were diluted, stored in SM buffer⁸ and used for routine plaquing assays. Plaque assays were conducted at 37 °C with 20 ml of bottom agar containing 10 mM MgSO₄ and 0.35% or 0.7% top agar (often both concentrations were used in parallel) also containing 10 mM MgSO₄ and any inducer molecules. Spots of 3 µl were applied to the top agar after it had been poured and solidified. For high-titre lysates to generate phage DNA, plates with a high number of plaques were flooded with SM buffer and collected⁸. The lysates were subsequently treated with DNase. Phage DNA was extracted with the Wizard Genomic DNA Purification Kit (Promega). DNA restriction assays were performed according to standard NEB protocols and restriction fragments were assessed by agarose gel electrophoresis.

Type I-C CRISPR–Cas system assay and expression in *P. aeruginosa* PAO1

Type I-C CRISPR–Cas function was tested by electroporating a strain that naturally contains I-C Cas genes (strain F11) with pHERD30T plasmids encoding crRNAs that target phages. To express this system heterologously in PAO1, the four effector Cas genes (*cas5*, *cas8* and *cas7*) were cloned into pUC18T-lac and inserted in the PAO1 chromosome as described above. After removal of the gentamicin marker, this strain was electroporated with the same pHERD30T crRNA-encoding plasmids to confirm function after induction with IPTG and arabinose.

Type I-F CRISPR–Cas system expression in *P. aeruginosa* PAO1

To express the type I-F system heterologously in PAO1, all I-F Cas genes (*cas1*, *cas3*, *csy1*, *csy2*, *csy3* and *csy4*) were cloned into pMMBHE plasmids and transformed into PAO1. Subsequently, this strain was electroporated with the pHERD30T crRNA-encoding plasmids to confirm function after induction with IPTG and arabinose. To maintain pHERD30T and pMMBHE in the same strain of *P. aeruginosa*, double selection of 30 µg ml⁻¹ gentamicin and 100 µg ml⁻¹ carbenicillin was used.

crRNA cloning and expression

All crRNAs used here were cloned into established entry vectors in the pHERD30T background. After removing a pre-existing Bsal cut site in the vector by mutagenesis, a pseudo-CRISPR array (that is,

repeat–spacer–repeat for types I, V or VI, or an sgRNA scaffold for type II) in which the spacing sequence possessed two inverted Bsal digest sites was then cloned into the vector, to facilitate scarless cloning of new spacers. Desired spacer sequences were chosen randomly across the phage genome (with the correct PAM sequence for the cognate CRISPR–Cas system) and ordered as two complementary oligonucleotides that generate sticky ends when annealed, to be cloned into the entry vector, which was digested with Bsal. Spacer oligonucleotides were treated with polynucleotide kinase (PNK), annealed and ligated into the entry vector.

SpyCas9 and sgRNA expression in *P. aeruginosa*

The *S. pyogenes cas9* gene was cloned into a pUC18T-Ara integration vector and then inserted into the attTn7 locus of PAO1. An sgRNA scaffold was constructed based on a previous design²⁶ with internal Bsal cut sites to enable insertion of pre-annealed oligos for scarless sgRNA design. This sgRNA scaffold was amplified with primers p30T-gRNA_Bsal and p30T-gRNA_Bsal_rev. The resulting product was inserted into the pHERD30T vector by Gibson assembly after backbone (pJW1) amplification by inverse PCR with primers gRNA_Bsal-p30T and gRNA_Bsal-p30T_rev. The sgRNA scaffold was positioned into pJW1 so that after Bsal cleavage the spacer insert +1 position would coincide with the pBAD transcription start site (TSS) +1 position. The resulting plasmid, pJB1, was digested with Bsal (NEB), followed by ligation of indicated pre-annealed oligonucleotides. Supplementary Table 3 contains a complete list of all target sequences. The sequence of the sgRNA construct with Bsal site locations is shown in Supplementary Table 3.

Cas9 in vitro cleavage

Cas9-based cleavage of the phage genome in vitro was conducted with purified Cas9 protein (NEB, M0386S), and the cleavage reaction based on Cas9-gRNA-tracrRNA was then performed according to the manufacturer's instructions (NEB). Cas9 crRNAs (Supplementary Table 3) were ordered as Alt-R CRISPR-Cas9 crRNAs from IDT and used without further modification. The tracrRNA was amplified using primers tracrRNA-FOR and tracrRNA-REV from a plasmid (pBR62). The tracrRNA was produced through a T7 RNAP reaction using dsDNA that encodes the tracrRNA downstream of a T7 RNAP promoter. Cas9 protein (NEB) was combined with pre-annealed crRNA and tracrRNA complex at a 1:1 molar ratio. For targeting KasI-liberated ΦKZ gDNA, 500 ng of ΦKZ DNA was co-incubated with Cas9 ribonucleoprotein (RNP), which cleaves at position 183,270, and KasI in NEB buffer 3.1 for 1 h. After stopping the reaction by proteinase K treatment, products were assessed by agarose gel electrophoresis. For Cas9 digestion of whole DNA, the reaction was performed at 37 °C for 4 h with 300 ng of ΦKZ or DMS3 gDNA and the products were assessed by agarose gel electrophoresis. Two Cas9 guides were selected that cleave at positions 158,649 and 168,715 of the ΦKZ genome to liberate a fragment of approximately 10 kb.

Cas12a and crRNA design for expression in *P. aeruginosa*

The humanized allele of the *cpf1* gene of *M. bovocalli* (MBO_03467, KDN25524.1) was sub-cloned from pTE4495 (Addgene) into pUC18T-lac using primers pUC_cpf1_F and pUC_cpf1_R and inserted in the PAO1 chromosome as described above. A Cpf1 repeat–spacer–repeat pseudo-CRISPR array was synthesized as oligonucleotides, annealed, ligated into a pHERD30T vector and digested with NcoI and HindIII. Spacer sequences were cloned into the resulting vector (pJB2) after digestion with Bsal and ligation of pre-annealed spacer oligonucleotide pairs.

Cas13a and crRNA design for expression in *P. aeruginosa*

The wild-type allele of the *cas13* gene of *L. seeligeri* and *Leptotrichia shahii* was sub-cloned from p2CT-His-MBP-Lse_C2c2_WT and p2CT-His-MBP-Lsh_C2c2_WT (Addgene) into pUC18T-lac. LseCas13 and LshCas13 were inserted in the PAO1 chromosome as described above. An Lse- and

an *LshCas13a* repeat–spacer–repeat pseudo-CRISPR array were synthesized as oligonucleotides, annealed, ligated into a pHERD30T vector and digested with *NcoI* and *EcoRI*. Spacer sequences were cloned into the resulting vectors (pSDM057 and pSDM070, respectively) after *BsaI* digestion and ligation of pre-annealed spacer oligonucleotide pairs. crRNA expression vectors were introduced into PAO1 tn7::*cas13^{lse}* and PAO1 tn7::*cas13^{sh}*. The resulting strains were assayed for phage sensitivity under standard phage plating conditions, with induction of both Cas13 and the gRNAs (50 µg ml⁻¹ gentamicin, 0.1% (L)-arabinose, 1 mM IPTG).

EcoRI expression in *P. aeruginosa*

The wild-type alleles of the M-EcoRI (methyltransferase) and R-EcoRI (endonuclease) genes were sub-cloned from pSB1A3 EcoRI Methylase-AmilCP and pSB1A3 EcoRI-RTX with EcoRI Methylase-AmilCP (Addgene plasmid 85166 and 85165), p2CT-His-MBP-Lse_C2c2_WT and p2CT-His-MBP-Lsh_C2c2_WT (Addgene) into pHERD30T using Gibson assembly. The resulting plasmids, pSDM160 and pSDM161, were electroporated into PAO1 Δ *hsdR* (SDM020). The resulting strains were assayed for phage sensitivity under standard phage plating conditions, with induction of both M-EcoRI (for genome protection) and R-EcoRI (50 µg ml⁻¹ gentamicin, 0.1% (L)-arabinose).

Restriction-modification assay

PAO1, PAK and PAO1 Δ *hsdR* were grown to saturation in LB at 37 °C. Then, 4 ml of 0.7% molten top agar with 10 mM MgSO₄ were seeded with 100 µl saturated culture and spread on 20 ml 10 mM MgSO₄ LB agar plates. Tenfold serial dilutions of bacteriophage JBD30 and Φ KZ propagated on strain PAO1 and PAK were spotted (2.5 µl) on plates. Plates were incubated at 37 °C overnight and imaged the following day.

Chromosomal knockout of *hsdR*

To delete *hsdR* (NP_251422.1) from the PAO1 genome, a PAO1 strain that expresses Cas9 from *S. pyogenes* was programmed to express an sgRNA against *hsdR*: GCCCTCATCGAAGAAACCAG. In addition, the pHERD30T plasmid expressing this sgRNA was engineered to carry a repair template. This repair template consisted of the 500 bp upstream of *hsdR* and the 500 bp downstream of *hsdR* directly enjoined to one another. Induction of Cas9 and sgRNA led to cellular toxicity, as measured by OD_{600nm} (data not shown). Survivors of Cas9-mediated targeting were isolated. The *hsdR* locus of survivors was then amplified by colony PCR with primers binding outside of the region encompassed by the repair template. Products were resolved by gel electrophoresis in a 1.0% agarose TAE gel at 100 V and visualized using the SYBR Safe DNA stain. Amplicons of a reduced size were then sequenced, which confirmed the chromosomal deletion of *hsdR*. A clone with the correct deletion, SDM020, was chosen for downstream experiments.

Construction of fusion proteins

Plasmids expressing Cherry alone, Cherry-Cas3, or Cherry-Cas8 (of type I-C and type I-F systems) and Cherry-TopA were constructed by Gibson assembly in the pHERD30T plasmid digested with *SacI* and *PstI*. These fusions have a GGAGGCGGTGGAGCC nucleotide (G-G-G-G-A amino acid) linker sequence in between them. *cherry* was amplified from SF-pSFFV-sfCherryFLIM3_TagBFP (provided by the laboratory of B. Huang, UCSF). *cas3* and *cas8* of the type I-C and type I-F systems were amplified from LL77 and PA14, respectively. *topA* was amplified from gDNA of PAO1. All of the primers that were used for the construction of the plasmids are listed in Supplementary Table 3.

Plasmids expressing Cherry–Cas9 (pESN28) (primers: prESN74, prESN75, prESN76, prESN77) and Cherry–Cas9–ORF152 (pESN29) (prESN80, prESN81, prESN82, prESN83) were constructed by Gibson assembly in the pHERD30T plasmid. Cherry–ORF152 (pESN32) (prESN91, prESN92) was constructed by PCR amplification to omit Cas9 and ligated using a KLD reaction. An SGAAAAGGSQK amino acid

linker connects Cherry to the other proteins. A GGGGS amino acid linker connects Cas9 and ORF152. The plasmid expressing cMyc–ORF152 (prESN153, prESN154) was constructed by PCR amplification (primers: prESN153 and prESN154) using the p30-Cas9-ORF152 plasmid as the template, followed by a PCR clean-up and KLD ligation to circularize. This removed Cas9 from the plasmid, and added cMyc. All plasmids were designed using SnapGene.

To construct translational fusions of proteins, desired gene fragments including *cas9*, M-EcoRI, R-EcoRI, *orf152* (NP_803718.1) and sfCherry2 were amplified by PCR from templates pHERD30T::Cas9, pSB1A3::M.EcoRI-AmilCP, pSB1A3::M.EcoRI-AmilCP;R.EcoRI-RTX, Φ KZ gDNA and pHERD30T::sfCherry2, respectively. pHERD30T was linearized by restriction digestion with *SacI*-HF and *PstI*-HF or by PCR. PCR primers included 15–30-bp overhangs for Gibson assembly. Overhangs that enjoin genes included amino acid linkers GGGGS or GGSGGS. PCRs were treated with *DpnI* to eliminate template DNA. All PCRs and restriction digests were purified using a PCR clean-up kit (Zymo Research DNA Clean and Concentrator Kits). Linearized vector and gene fragments were treated with Gibson assembly, and Gibson assembly reactions were transformed into competent *E. coli*. Plasmid products were isolated by miniprep and submitted for sequencing. Correct assemblies were electroporated into appropriate *P. aeruginosa* strains.

Isolation of Cas13 escapers

For identifying escapers of Cas13a RNA targeting, 3 µl of high-concentration Φ KZ lysates was mixed with 150 µl of overnight cultures of SDM078, SDM109 or SDM107 (strains expressing *Cas13a* and a gRNA against Φ KZ). After incubating at 37 °C for 10 min, samples were mixed with 4 ml of 0.7% agar, 10 mM MgSO₄, 1 mM IPTG and 0.1% arabinose and plated in LB agar plates with gentamicin (50 µg ml⁻¹). After overnight incubation, plates were examined for the presence of escaper plaques. Escapers were formed in SDM078 and SDM109, but not in SDM107. Ten phages that escaped targeting from SDM078 and SDM109 were purified and the protospacer locus was amplified using PCR and subsequently sequenced. Six unique outcomes were identified and shown in Fig. 4.

Growth curve experiments

Growth curve experiments were carried out in a Synergy H1 microplate reader (BioTek, with Gen5 software). Cells were diluted 1:100 from a saturated overnight culture with 10 mM MgSO₄ and antibiotics and inducers, as appropriate. Diluted culture (140 µl) was added together with 10 µl of phage to wells in a 96-well plate. This plate was cultured with maximum double orbital rotation at 37 °C for 24 h with OD_{600nm} measurements every 5 minutes.

Immunofluorescence

Sample growth. Overnight cultures (5 ml) of a strain expressing Cas9 and an sgRNA targeting Φ KZ (SDM065), and a strain expressing cMyc–ORF152 (bESN27), were grown at 30 °C in LB medium with gentamicin. A 1:30 back dilution of the overnight culture into LB was grown at 30 °C for 1 h. Protein and guide expression was induced with 0.1% arabinose and 0.5 mM IPTG, respectively. After 1 h of expression, an aliquot of uninfected cells was fixed and the remaining cultures were infected with Φ KZ using a MOI of 1.5. Infected cell aliquots were collected and fixed at 60 min post-infection.

Fixation. This protocol was adapted from a previous study²⁷. Samples were fixed with 5× fixing solution (12.5% paraformaldehyde, 150 mM KPO₄ pH 7.2) and incubated for 15 min at room temperature, followed by 20 min on ice. Samples were then washed in PBS three times and finally resuspended in GTE (50 mM glucose, 10 mM EDTA pH 8.0, 20 mM Tris-HCl pH 7.65) with 10 µg ml⁻¹ lysozyme. Resuspended cells were transferred to polylysinated coverslips and dried. Once dry, the coverslips were incubated in cold methanol for 5 min and cold acetone for 5 min. Cells were rehydrated by a rinse in PBS, followed by a 3-min

Article

incubation in PBS with 2% BSA blocking solution. Cells were incubated with a 1:50 dilution of primary antibody (Cas9 (7A9-3A3): sc-517386 or cMyc (9E10): sc-40) in PBS with 2% BSA for 1 h, followed by 3 washes of 7 min each in fresh PBS with 2% BSA. Coverslips were then incubated in the dark for 1 h with secondary antibody (goat anti-mouse Alexa Fluor 555, Life Technologies A-21424) diluted 1:500 in PBS with 2% BSA. DAPI was added for the final 10 min of the incubation. Cells were washed in PBS 3 times for 7 min. Coverslips were then placed on slides using mounting medium (v/v 90% glycerol, v/v 10% Tris pH 8.0 and w/v 0.5% propyl-gallate) and sealed with clear nail polish.

Microscopy and analysis. Images were collected using a Zeiss Axiovert 200M microscope, and were processed using NIS Analysis software at the UCSF Nikon Imaging Center. Compartments and cells were manually selected using the Simple ROI Editor. Background subtractions were conducted for each cell and compartment separately. The corrected intensities for the cytoplasmic and compartment regions were averaged over the area of each cell and compartment using Matlab and plotted using GraphPad Prism 6. Data from two pooled replicates were fitted with a line, with 95% confidence intervals shown as dashed lines. The slope is as reported in the plots.

Live-cell imaging

For live-cell imaging of Φ KZ infection, freshly grown cells from LB plates were picked and resuspended in 100 μ l of LB medium. Around 5–10 μ l of the samples was spotted on 0.85% agarose pads with 1:5 diluted LB, arabinose (0.01–0.05%) and DAPI (2 μ g ml⁻¹). Samples were then incubated in a humidified chamber and allowed to grow for 3 h at 30 °C. Φ KZ lysate (5 μ l) was spotted on top of the agar pad and the samples were grown for an additional 1 h. Cells were visualized in the microscope after being covered with a cover slip. A Nikon Ti2-E inverted microscope equipped with the Perfect Focus System (PFS) and a Photometrics Prime 95B 25-mm camera were used for live-cell imaging. Images were processed using NIS Elements AR software.

Reporting summary

Further information on research design is available in the Nature Research Reporting Summary linked to this paper.

Data availability

All data generated or analysed during this study are included in this published article and its Supplementary Information files.

25. Choi, K.-H. & Schweizer, H. P. mini-Tn7 insertion in bacteria with single attTn7 sites: example *Pseudomonas aeruginosa*. *Nat. Protoc.* **1**, 153–161 (2006).
26. Jinek, M. et al. A programmable dual-RNA-guided DNA endonuclease in adaptive bacterial immunity. *Science* **337**, 816–821 (2012).
27. Cowles, K. N. et al. The putative POC complex controls two distinct *Pseudomonas aeruginosa* polar motility mechanisms. *Mol. Microbiol.* **90**, 923–938 (2013).

Acknowledgements Research in the J.B.-D. laboratory was supported by the University of California San Francisco Program for Breakthrough in Biomedical Research, which is funded in part by the Sandler Foundation, and an NIH Office of the Director Early Independence Award (DP5-OD021344 (J.B.-D.) and R01-GM127489 (J.B.-D.)). This work was also supported by HHMI (D.A.A.) and NIH grants R35GM118099 (D.A.A.) and GM104556 (D.A.A., J.P.). Φ KZ, JBD30, JBD68, D3 and F8 were provided by the laboratory of A. Davidson and Φ PA3 by the D.A.A. laboratory; phage DMS3m was a gift from G. O'Toole; the *S. pyogenes* cas9 expression plasmid for integration in the PAO1 chromosome was from J. M. Peters and C. A. Gross; pTE4495 (MbCpf1/MbCas12a) (Addgene plasmid 80339) was a gift from E. Welker; LseCas13a (Addgene plasmid 83486) was a gift from J. Doudna; pSB1A3 EcoRI Methylase-Ami1CP and pSB1A3 EcoRI-RTX with EcoRI Methylase-Ami1CP (Addgene plasmids 85166 and 85165) were gifts from R. Dowell; and the type I-F crRNA expression plasmid pABO4 was from A. Borges (J.B.-D. laboratory).

Author contributions S.D.M. constructed strains and performed experiments relating to restriction modification, relocalization of enzymes, Cas13, Cas12 and all liquid infection assays, and prepared figures. E.S.N. performed fluorescence microscopy experiments with guidance from V.C. and J.P., and strain construction and data analysis under the supervision of D.A.A. S.G. performed microscopy experiments, strain construction, plaque assays, data analysis, in vitro digestion assays and Cas13 escaper experiments. L.M.L. performed type I-C Cas3 experiments. J.D.B. constructed and performed experiments with Cas9-expressing strains and performed in vitro digestion assays. A.T. isolated and sequenced Cas13 escaper phages. J.B.-D. conceived the project, performed Cas3 and Cas9 experiments, supervised all experiments and wrote the manuscript together with S.D.M. All authors edited the manuscript.

Competing interests J.B.-D. is a scientific advisory board member of SNIPR Biome and Excision Biotherapeutics and a scientific advisory board member and co-founder of Acrigen Biosciences.

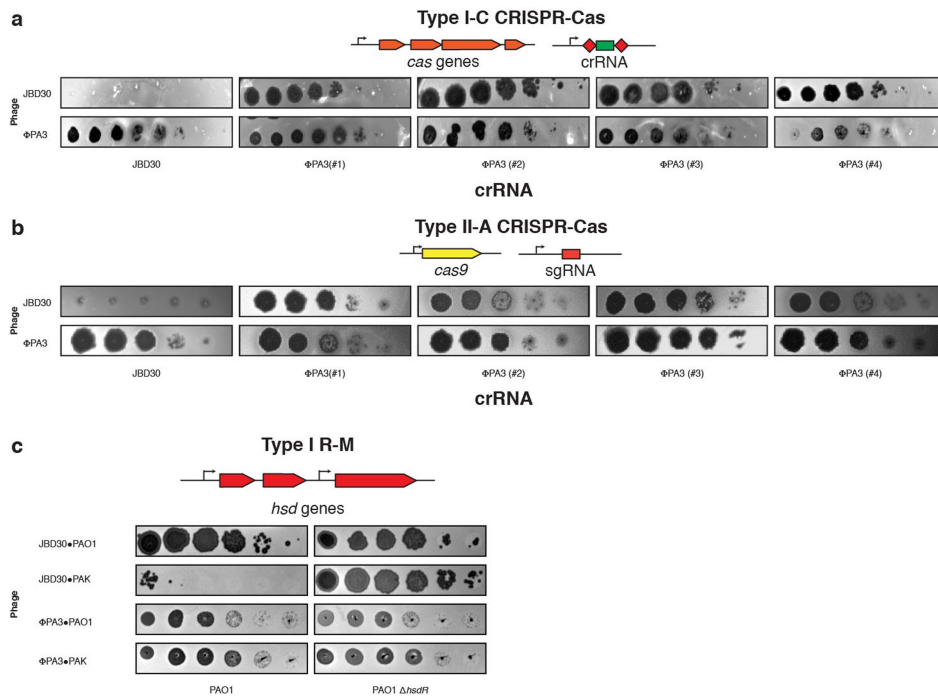
Additional information

Supplementary information is available for this paper at <https://doi.org/10.1038/s41586-019-1786-y>.

Correspondence and requests for materials should be addressed to J.B.-D.

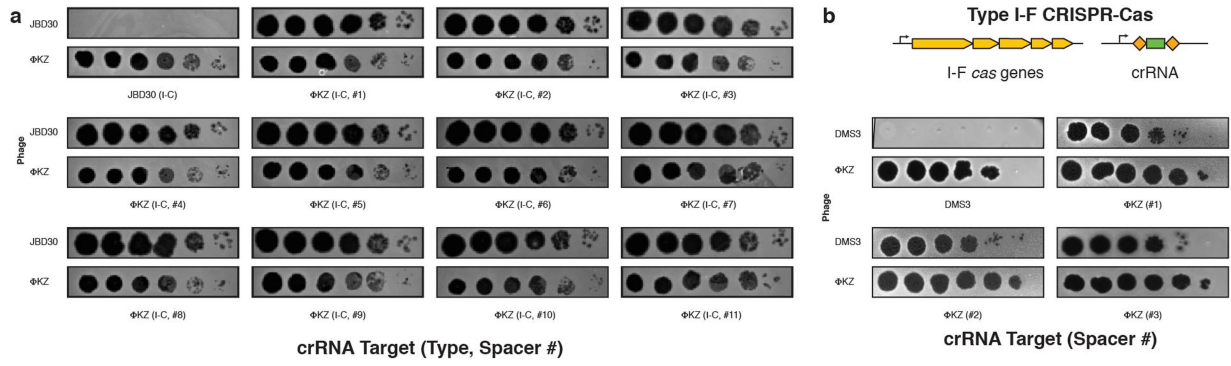
Peer review information Nature thanks Eugene Koonin and the other, anonymous, reviewer(s) for their contribution to the peer review of this work.

Reprints and permissions information is available at <http://www.nature.com/reprints>.



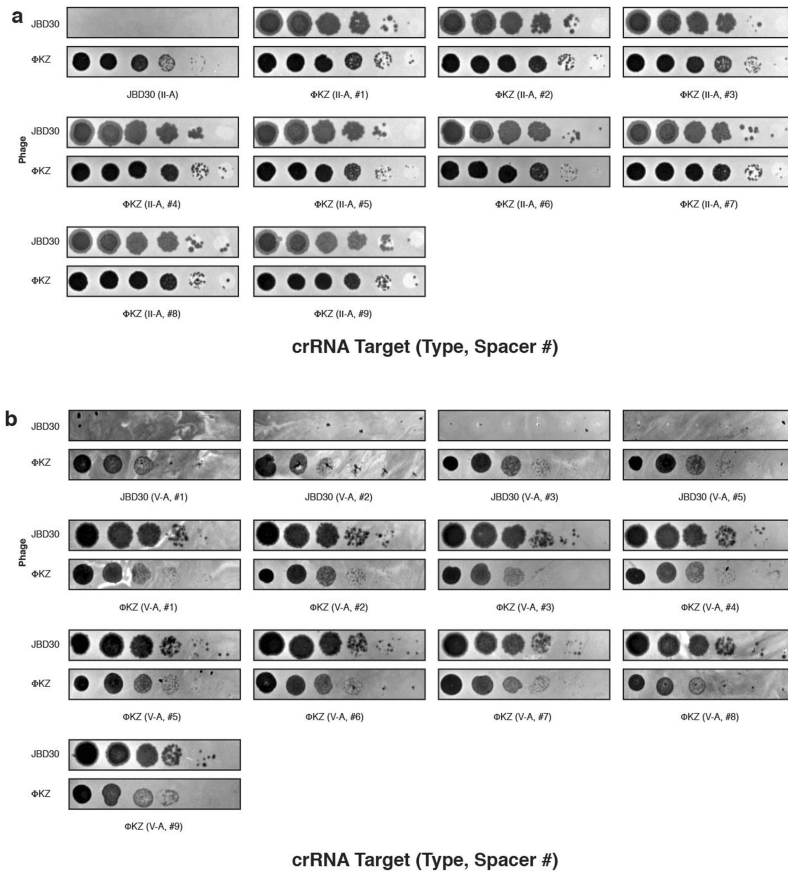
Extended Data Fig. 1 | Jumbo phage Φ PA3 resists targeting by CRISPR-Cas systems and an R-M system. **a**, Strain PAO1 was engineered to express the type I-C Cas genes and distinct crRNAs that target the indicated phages. **b**, Strain PAO1 was engineered to express the type II-A Cas9 protein and distinct sgRNAs that target the indicated phages. **c**, The endogenous type I R-M system

(hsdRSM) in wild-type PAO1 and a mutant strain with an isogenic *hsdR* knockout (PAO1 Δ *hsdR*) was assayed using phages that were propagated on PAO1 or PAK as indicated, and strains were subjected to a plaque assay. All plaque assays were conducted as in Fig. 1a and were replicated twice with similar results.



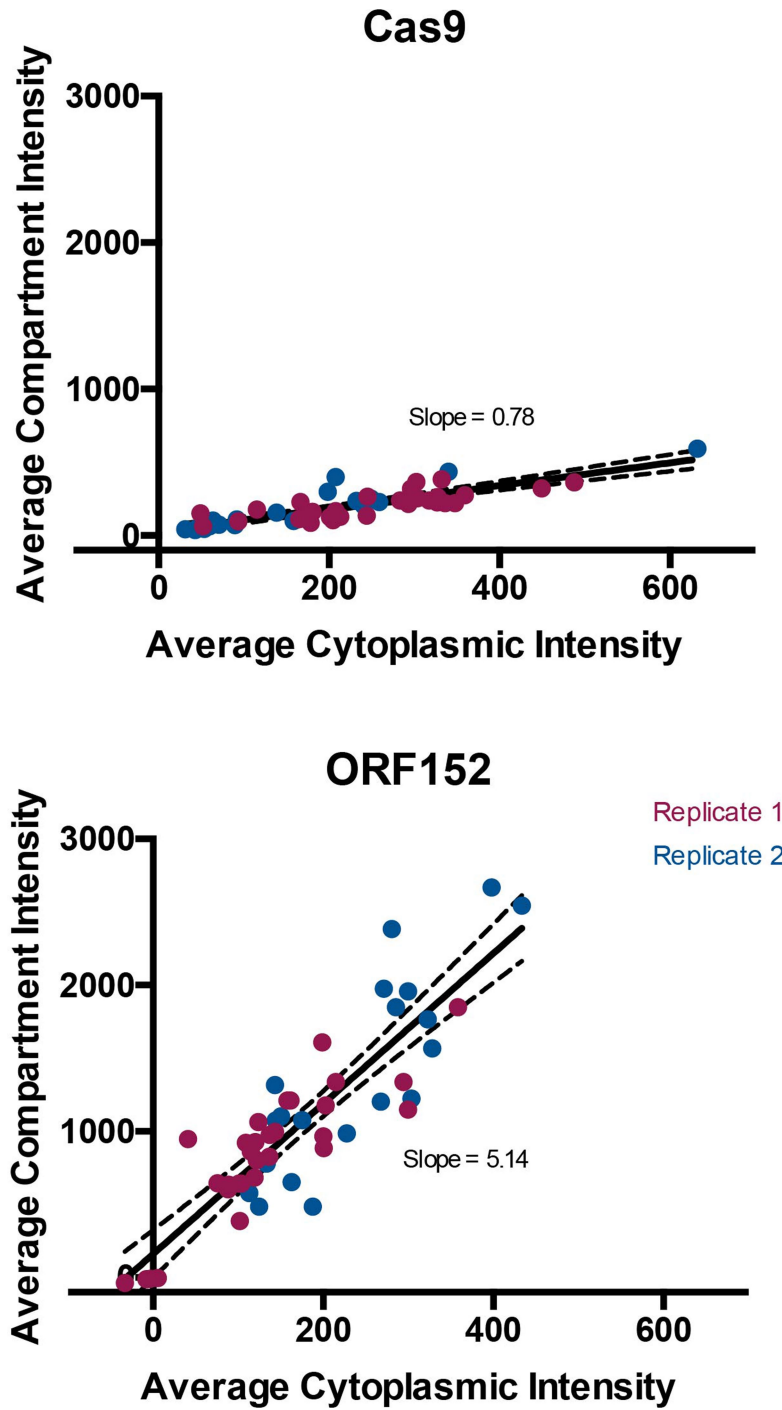
Extended Data Fig. 2 | Phage Φ KZ resists *P. aeruginosa* type I-C and type I-F CRISPR-Cas immunity. **a**, Strain PAO1 was engineered to express the type I-C Cas genes and distinct crRNAs that target phage JBD30 and phage Φ KZ. **b**, Strain PAO1 was engineered to express the type I-F Cas genes and distinct

crRNAs that target phage JBD30 and phage Φ KZ. All plaque assays were conducted as in Fig. 1a and were replicated two or more times with similar results.

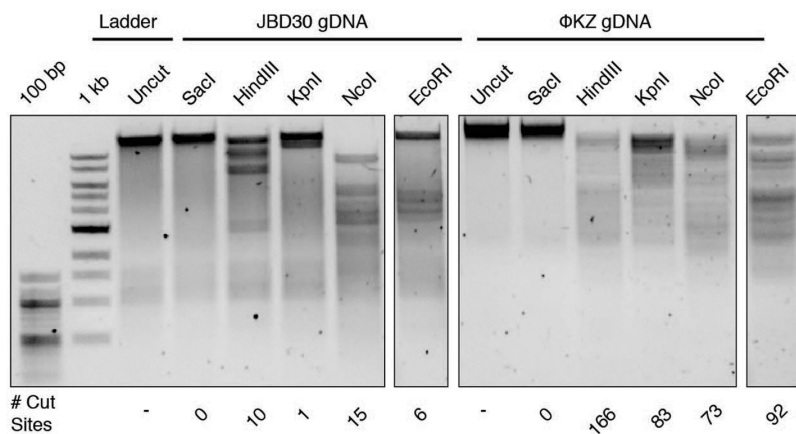


Extended Data Fig. 3 | Phage Φ KZ resists targeting by heterologous type II-A and V-A CRISPR-Cas systems. **a**, Strain PAO1 was engineered to express the type II-A Cas9 protein and distinct sgRNAs that target the indicated phages. **b**, Strain PAO1 was engineered to express the type V-A Cas12a protein and

distinct crRNAs against the indicated phages. All plaque assays were conducted as in Fig. 1a and were replicated two or more times with similar results.

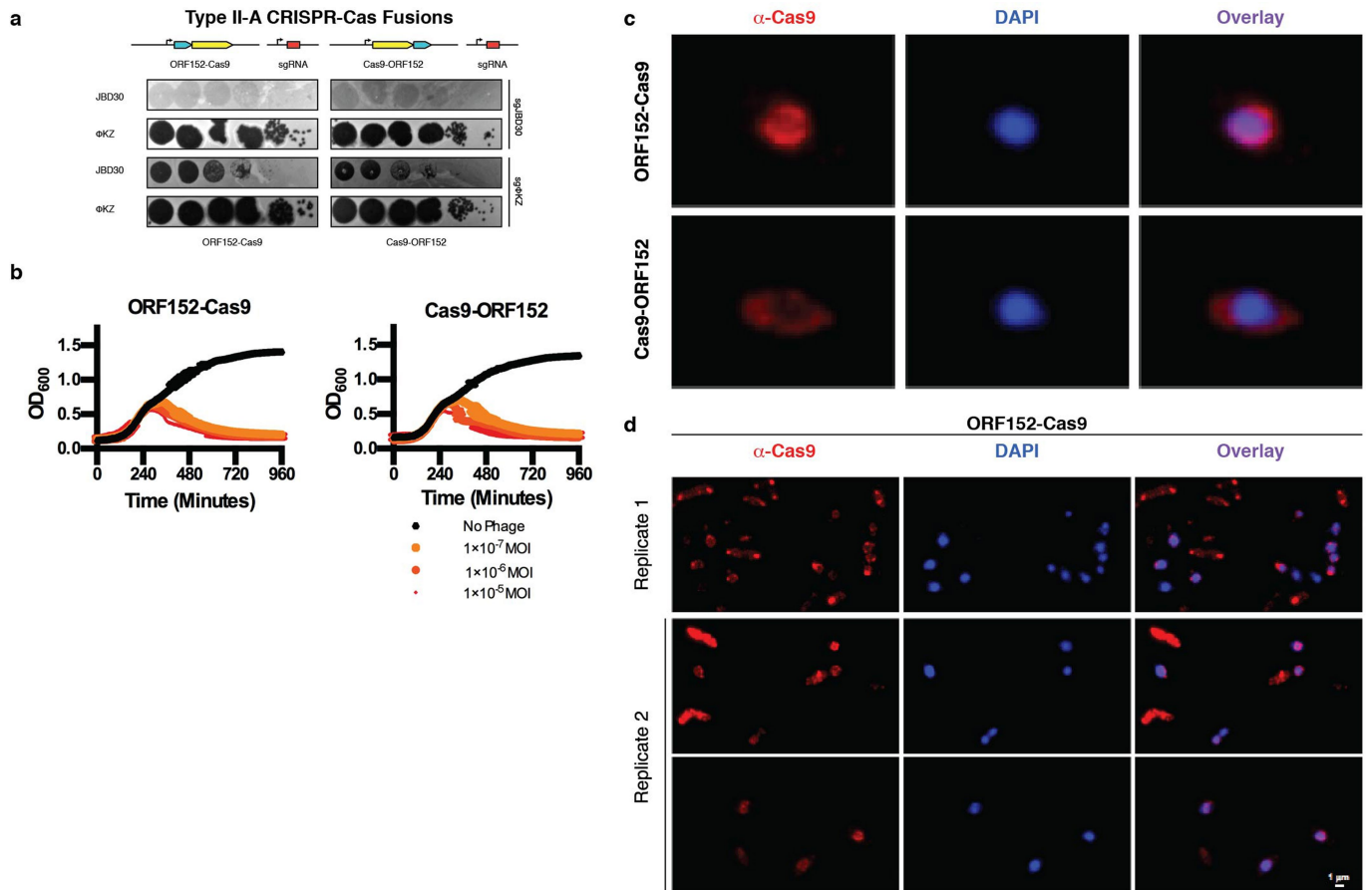


Extended Data Fig. 4 | Quantification of Cas9 localization during phage Φ KZ infection of *P. aeruginosa*. The localization of Cas9 and ORF152 in the cytoplasm and shell during Φ KZ infection was quantified. Data points (individual cells) from two pooled replicate experiments are fitted with a line and 95% confidence intervals are indicated with dashed lines. The slope is as reported in the plots.



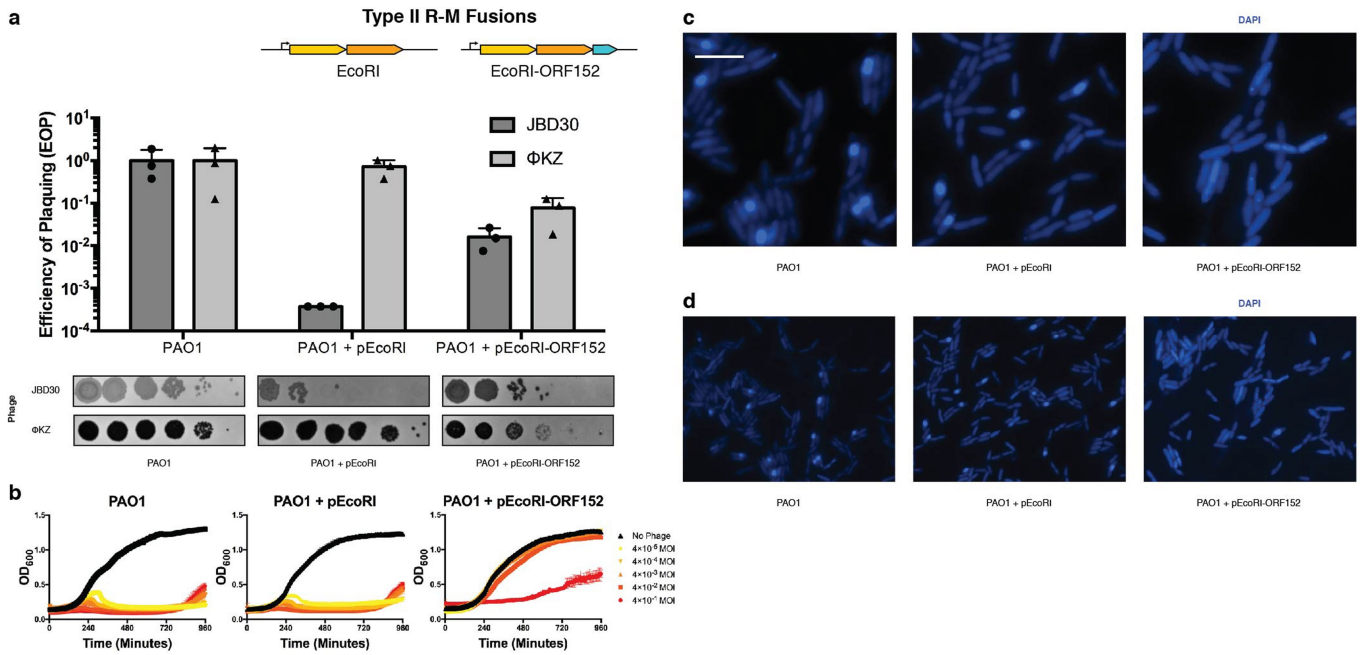
Extended Data Fig. 5 | Phage Φ KZ gDNA is susceptible in vitro to cleavage by restriction endonucleases. gDNA was isolated from phages Φ KZ and JBD30 and subjected to digestion with the indicated restriction enzymes in vitro. The

number of cut sites for each enzyme is shown at the bottom of the gels. Products were visualized on a 0.7% agarose gel stained with SYBR Safe. The experiment was replicated twice with similar result.



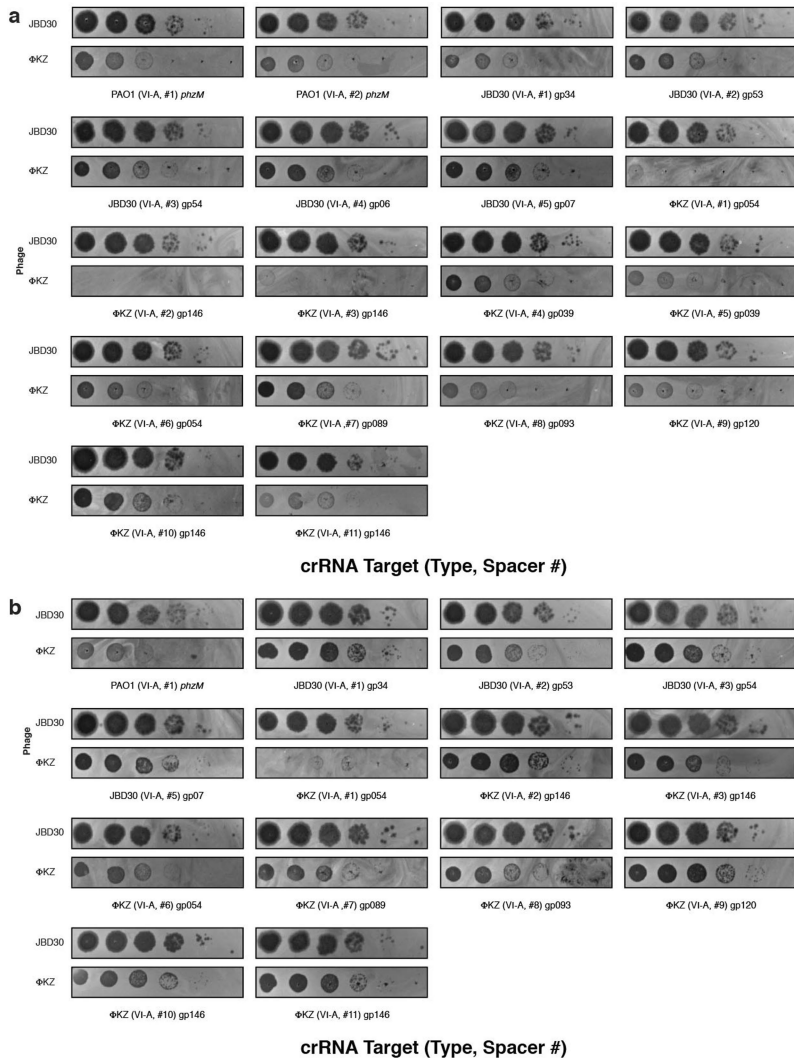
Extended Data Fig. 6 | Cas9 protein fused to ORF152 localizes to the periphery of the shell, but does not enable immune activity against Φ KZ.
a, Strain PAO1 was engineered to express Cas9 fused to ORF152 at either the N or the C terminus, with sgRNAs targeting the indicated phages. **b**, Growth curves measuring the OD_{600nm} of PAO1 cells that were infected with Φ KZ at the indicated MOI. **c**, Fluorescence microscopy of PAO1 fusion strains, immunostained for Cas9, in cells that express ORF152-Cas9 or Cas9-ORF152.

d, Fluorescence microscopy of *P. aeruginosa*, immunostained for Cas9, in cells that express ORF152-Cas9. The DAPI stain in **c**, **d** shows the phage DNA within the shell. All plaque assays were conducted as in Fig. 1a and were replicated four times with similar results. The growth curve experiments (**b**) were replicated three times with similar results. Microscopy (**c**, **d**) was replicated twice with similar results.



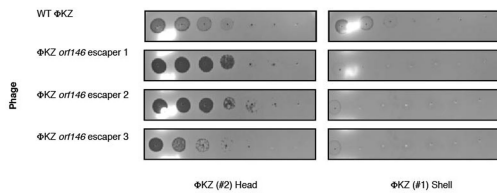
Extended Data Fig. 7 | Fusion of EcoRI restriction enzymes to ORF152 enables immune activity. **a**, Strain PAO1 was engineered to express EcoRI or an EcoRI-ORF152 fusion protein. Plaque assays were conducted as in Fig. 1a and quantified ($n = 3$). **b**, Growth curves measuring the OD_{600nm} of PAO1 cells that were infected with ΦKZ at the indicated MOI. **c**, **d**, Live-cell fluorescence

imaging (with a wide field of view in **d**) of *P. aeruginosa* strains that were engineered to express EcoRI or EcoRI-ORF152. The DAPI stain shows the phage DNA. All plaque assays were replicated three times with similar results. The growth curve experiments (**b**) were replicated twice with similar results. Microscopy (**c**, **d**) was replicated twice with similar results. Scale bar, 5 μm .

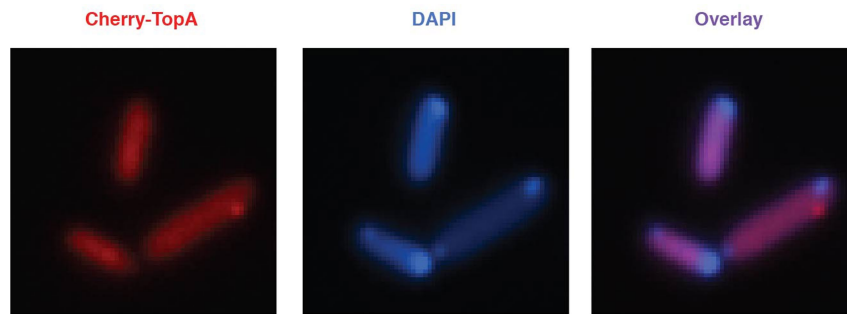


Extended Data Fig. 8 | Phage ΦKZ is sensitive to RNA targeting with Cas13.
a, Strain PAO1 expressing *LseCas13a* and distinct crRNAs that target the indicated genes. **b**, Strain PAO1 expressing *LshCas13a* and distinct crRNAs that

target the indicated genes. All plaque assays were conducted as in Fig. 1a and were replicated twice with similar results.



Extended Data Fig. 9 | Phage ΦKZ escaper mutants are selected by Cas13-mediated RNA targeting. Strain PAO1 expressing *LseCas13a* and a crRNA that targets the indicated gene. Plaque assays were conducted as in Fig. 1a using wild-type and escaper-mutant ΦKZ. Wild-type ΦKZ is targeted by both strains and the faint clearings observed here are not observed as plaques in a full-plate assay. All plaque assays were replicated twice with similar results.



Extended Data Fig. 10 | Observation of DAPI-stained phage DNA adjacent to a nascent shell that contains Cherry-TopA. Live-cell fluorescence imaging of *P. aeruginosa* strains that were engineered to express Cherry-TopA and

infected with Φ KZ. The DAPI stain labels DNA. Microscopy was replicated three times with similar results.

Reporting Summary

Nature Research wishes to improve the reproducibility of the work that we publish. This form provides structure for consistency and transparency in reporting. For further information on Nature Research policies, see [Authors & Referees](#) and the [Editorial Policy Checklist](#).

Statistics

For all statistical analyses, confirm that the following items are present in the figure legend, table legend, main text, or Methods section.

n/a Confirmed

- | | | |
|-------------------------------------|-------------------------------------|--|
| <input type="checkbox"/> | <input checked="" type="checkbox"/> | The exact sample size (n) for each experimental group/condition, given as a discrete number and unit of measurement |
| <input type="checkbox"/> | <input checked="" type="checkbox"/> | A statement on whether measurements were taken from distinct samples or whether the same sample was measured repeatedly |
| <input type="checkbox"/> | <input checked="" type="checkbox"/> | The statistical test(s) used AND whether they are one- or two-sided
<i>Only common tests should be described solely by name; describe more complex techniques in the Methods section.</i> |
| <input checked="" type="checkbox"/> | <input type="checkbox"/> | A description of all covariates tested |
| <input checked="" type="checkbox"/> | <input type="checkbox"/> | A description of any assumptions or corrections, such as tests of normality and adjustment for multiple comparisons |
| <input checked="" type="checkbox"/> | <input type="checkbox"/> | A full description of the statistical parameters including central tendency (e.g. means) or other basic estimates (e.g. regression coefficient) AND variation (e.g. standard deviation) or associated estimates of uncertainty (e.g. confidence intervals) |
| <input checked="" type="checkbox"/> | <input type="checkbox"/> | For null hypothesis testing, the test statistic (e.g. F , t , r) with confidence intervals, effect sizes, degrees of freedom and P value noted
<i>Give P values as exact values whenever suitable.</i> |
| <input checked="" type="checkbox"/> | <input type="checkbox"/> | For Bayesian analysis, information on the choice of priors and Markov chain Monte Carlo settings |
| <input checked="" type="checkbox"/> | <input type="checkbox"/> | For hierarchical and complex designs, identification of the appropriate level for tests and full reporting of outcomes |
| <input checked="" type="checkbox"/> | <input type="checkbox"/> | Estimates of effect sizes (e.g. Cohen's d , Pearson's r), indicating how they were calculated |

Our web collection on [statistics for biologists](#) contains articles on many of the points above.

Software and code

Policy information about [availability of computer code](#)

Data collection

Pictures of plaque assays and gels were taken using Image Lab (TM) Version 6.0.1 (C) 2017, Bio-Rad Laboratories, Inc. Growth curve assays were collected using BioTek Synergy H1 software Gen5 3.05.11. Microscopy was collected using NIS Elements-AR software 5.0.2.00.

Data analysis

Pictures of plaque assays and gels were edited using Image Lab (TM) Version 6.0.1 (C) 2017, Bio-Rad Laboratories, Inc. and ImageJ 1.50i. Plate reader growth curves were plotted using Prism 6. Plaque assay quantification was plotted using Prism 6. For Cas9 exclusion quantification, cells and compartments were chosen using Simple ROI Editor, from NIS Elements-AR 5.0.2.00. Background subtraction and average intensities were performed using MatLAB R2018b 9.5.0.944444 and plotted using Prism 6.

For manuscripts utilizing custom algorithms or software that are central to the research but not yet described in published literature, software must be made available to editors/reviewers. We strongly encourage code deposition in a community repository (e.g. GitHub). See the Nature Research [guidelines for submitting code & software](#) for further information.

Data

Policy information about [availability of data](#)

All manuscripts must include a [data availability statement](#). This statement should provide the following information, where applicable:

- Accession codes, unique identifiers, or web links for publicly available datasets
- A list of figures that have associated raw data
- A description of any restrictions on data availability

Included in main text.

Field-specific reporting

Please select the one below that is the best fit for your research. If you are not sure, read the appropriate sections before making your selection.

Life sciences Behavioural & social sciences Ecological, evolutionary & environmental sciences

For a reference copy of the document with all sections, see [nature.com/documents/nr-reporting-summary-flat.pdf](https://www.nature.com/documents/nr-reporting-summary-flat.pdf)

Life sciences study design

All studies must disclose on these points even when the disclosure is negative.

Sample size	For I-C, I-F, II-A, V-A, and VI-A CRISPR and type I and type II restriction enzyme plaque assays, $n \geq 2$ as output of targeting was either full plaque formation or complete protection and thus was not quantified. For II-A and VI-A CRISPR growth curve assays, $n=3$. For EcoRI Fusion plaque assays, $n=3$. For EcoRI Fusion growth curve assay, $n=3$. For microscopy, one sample was imaged and representative cells are demonstrated. For immunofluorescence quantification, two replicates were imaged and selected cells were chosen ($n=30$ for Replicate 1, $n=20$ for Replicate 2) and analyzed.
Data exclusions	Gels in Figure 3 and Extended Figure 5 were cropped for clarity and conciseness. Full gels are provided in a .pdf.
Replication	Plaque assays and growth curves were all performed at least twice, showing replication each time. Here we show representative examples. Microscopy data shown is representative examples of phenotypes observed throughout the sample(s).
Randomization	Samples were organized into experimental groups depending on genotype, including genes and crRNAs encoded by the bacterial strain. Randomization was not performed in this study.
Blinding	Blinding was not performed in this study, as it was not relevant given that all results are quantitative, or represent binary states (e.g. exclusion vs. inclusion).

Reporting for specific materials, systems and methods

We require information from authors about some types of materials, experimental systems and methods used in many studies. Here, indicate whether each material, system or method listed is relevant to your study. If you are not sure if a list item applies to your research, read the appropriate section before selecting a response.

Materials & experimental systems

n/a	Involvement in the study
<input type="checkbox"/>	<input checked="" type="checkbox"/> Antibodies
<input checked="" type="checkbox"/>	<input type="checkbox"/> Eukaryotic cell lines
<input checked="" type="checkbox"/>	<input type="checkbox"/> Palaeontology
<input checked="" type="checkbox"/>	<input type="checkbox"/> Animals and other organisms
<input checked="" type="checkbox"/>	<input type="checkbox"/> Human research participants
<input checked="" type="checkbox"/>	<input type="checkbox"/> Clinical data

Methods

n/a	Involvement in the study
<input checked="" type="checkbox"/>	<input type="checkbox"/> ChIP-seq
<input checked="" type="checkbox"/>	<input type="checkbox"/> Flow cytometry
<input checked="" type="checkbox"/>	<input type="checkbox"/> MRI-based neuroimaging

Antibodies

Antibodies used	Santa Cruz Biotechnology, Inc. Cas9 (7A9-3A3): sc-517386, Santa Cruz Biotechnology, Inc cMyc Antibody (9E10): sc-40
Validation	Cas9, from the manufacturer's website: "Yes, this mouse monoclonal antibody, Cas9 (7A9-3A3): sc-517386, has been validated to work for immunofluorescent staining applications. Unfortunately, we do not yet have any published IF data for this clone on our website. However, this clone, (7A9-3A3) has been widely published in the literature for use in a variety of applications, including IF." cMyc: There are 5553 citations of this antibody from Santa Cruz in the literature and several examples of both western blots and IF on the product website. But they do not specifically address validation of it anywhere.